

# Solvent Effects on Linear and Nonlinear Optical Properties of Donor–Acceptor Polyenes: Investigation of Electronic and Vibrational Components in Terms of Structure and Charge Distribution Changes

Roberto Cammi,<sup>†</sup> Benedetta Mennucci,<sup>‡</sup> and Jacopo Tomasi<sup>\*,‡</sup>

Contribution from the Dipartimento di Chimica Generale ed Inorganica, Università di Parma, viale delle Scienze, 43100 Parma, Italy, and Dipartimento di Chimica e Chimica Industriale, Università di Pisa, via Risorgimento 35, 56126 Pisa, Italy

Received March 12, 1998. Revised Manuscript Received June 22, 1998

**Abstract:** We investigate the influence of solvation media upon the relationship among structure, spatial distribution of electron density, and linear and nonlinear electric properties for two series of push–pull  $\pi$ -conjugated molecules. The analysis is performed on both electronic and vibrational components of static polarizability and first hyperpolarizability, and the effects solvent induce on them are analyzed singularly within the framework of the polarization continuum model. Solvent is found to affect the extent of charge separation induced in the ground state of these molecules. This charge separation leads to a geometric distortion, measured by the bond-length-alternation (BLA) parameter, which shows a solvent-induced evolution of the molecular geometry from a neutral, bond-alternated polyene-like structure, to a partially ionic cyanine-like structure, and ultimately to an ionic bond-alternated structure. As a consequence large changes in the linear and nonlinear response properties are found, in both their electronic and vibrational contributions. Regarding the latter, we recall that studies on vibrational (hyper)polarizabilities for molecular systems in solution are presented here for the first time.

## 1. Introduction

In the last few years, numerous theoretical efforts have been devoted to the computation of (hyper)polarizabilities of molecular and polymeric systems;<sup>1</sup> this is in fact a very active field of research being directly related to the design of new compounds for nonlinear optics (NLO) applications. Accurate ab initio quantum chemistry studies in this field provide efficient tools to understand the physical bases beyond the phenomena and to derive structure–property relationships, in addition to offer a reliable comparison with experimental data. Until very recently, most of these studies have focused on the electronic (hyper)polarizabilities; actually, the global effect of an applied external electrical field on a given molecular system has to be seen in terms of distortions both in the electronic charge distribution (i.e., the field acts as a source of electronic response) and in the nuclear motions which lead to vibrational contributions to (hyper)polarizabilities.

The necessity to take into account vibrational components, which was first recognized many years ago, has recently received a new great consideration, especially thanks to the works of Professor Bishop (for the moment we limit ourselves to quote two reviews, one published in the early 1990s<sup>2</sup> and the other quite recent,<sup>3</sup> but other papers will be given in the

following). This new interest originated an important development in theoretical studies on electric response functions so that, nowadays, papers in this field at least have to mention that, in addition to variations in the electronic charge distribution of the molecular system, there will be a change in its equilibrium geometry and, as a result of there being a different potential-energy curve or surface in the presence of the field, a change in the vibrational motion.

The question of vibration involves much more than the usual requirement of averaging an electronic property over the vibrational motion, e.g., the zero-point vibrational correction (ZPC), which usually changes (hyper)polarizability values by roughly a few percent; it contributes with a specific term to each (hyper)polarizability value. As a matter of fact the full vibrational contribution can be decomposed into two distinct components,<sup>4,5</sup> the “curvature” (curv) related to the field-dependent vibrational frequencies (i.e., the changes in the potential energy surface) and including the ZPC contribution, and the “nuclear relaxation” (nr) originated from the field-induced nuclear relaxation (i.e., the shift of the equilibrium geometry).

Although accurate numerical calculations of vibrational (hyper)polarizabilities have been carried out for molecular systems in vacuo,<sup>6–9</sup> no studies of the solvent effect on these

\* Corresponding author. E-mail: tomasi@dcci.unipi.it.

<sup>†</sup> Università di Parma.

<sup>‡</sup> Università di Pisa.

(1) (a) *Special Issue on Molecular Nonlinear Optics*; Ratner, M.A., Ed. *Int. J. Quantum Chem.* **1992**, *43*. (b) *Optical Nonlinearities in Chemistry*; Burland, D. M., Ed. *Chem. Rev.* **1994**, *94*. (c) *Modern Nonlinear Optics*; Evans, M., Kielich, S., Eds. *Adv. Chem. Phys.* **1993**, *85*.

(2) Bishop, D. M. *Rev. Mod. Phys.* **1990**, *62*, 343.

(3) Bishop, D. M. *Adv. Chem. Phys.*, in press.

(4) Martí, J.; Andrés, J. L.; Bertrán, J.; Duran, M. *Mol. Phys.* **1993**, *80*, 625.

(5) Martí, J.; Bishop, D. M. *J. Chem. Phys.* **1993**, *99*, 3860.

(6) Bishop, D. M.; Kirtman, B.; Kurtz, H. A.; Rice, J. E. *J. Chem. Phys.* **1993**, *98*, 8024.

(7) Duran, M.; Andrés, J. L.; Lieder, A.; Bertrán, J. *J. Chem. Phys.* **1989**, *90*, 328.

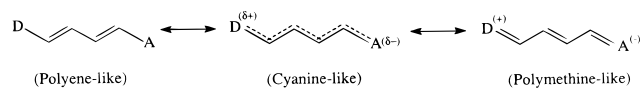


**Figure 1.** Resonance structures of a prototypical push–pull system.

quantities have appeared yet. All the papers on ab initio calculations of linear and nonlinear properties of molecular solutes immersed in liquid solvents refer in fact to electronic contributions only (see refs 10–13), eventually with inclusion of the ZPC contribution.<sup>14</sup> This paper is then the first attempt dealing with ab initio evaluation of vibrational static polarizability and first polarizability of molecular systems in solution.

The selected systems for the present study belong to the category of push–pull  $\pi$ -conjugated molecules, i.e., systems where a conjugated linker segment is capped by a donor group on one end and an acceptor on the other. Many donors and acceptors, as well as conjugated linkers of various nature and length, have been investigated both theoretically and experimentally.<sup>15–17</sup> The specificity of this kind of molecule, in particular we shall focus on substituted polyenes, is that their ground-state (GS) structure can be represented as a combination of different resonance forms, differing in the extent of charge separation (see Figure 1).

When the donor and acceptor groups are weak, the neutral polyene-like resonance form dominates the ground state and the molecule has a structure with a distinct alternation in the bond length between neighboring carbon atoms, i.e., a high degree of bond length alternation (BLA), defined as the difference between average single and double bond distances in the conjugated pathway. When donor and acceptor substituents become stronger, the contribution of ionic resonance forms to the ground state increases, and BLA first decreases until almost zero values (in the intermediate cyanine-like structure with partial charge separation) and then increases again toward the high negative values proper of the fully charge-separated polymethine-like (or zwitterionic) form. The relative contribution of these three resonance forms to the GS is also controlled by the polarity of the solvent in which the chromophore is dissolved; a more polar solvent increases the GS state polarization, which makes the partial and/or complete ionic forms more important.

Experiments have clearly demonstrated that the medium influences both the molecular geometry and the electronic charge

(8) Cohen, M. J.; Willets, A.; Amos, R. D.; Handy, N. C. *J. Chem. Phys.* **1994**, *100*, 4467.

(9) (a) Champagne, B.; Perpète, E. A.; André, J. M. *J. Chem. Phys.* **1994**, *101*, 10796. (b) Champagne, B.; Perpète, E. A.; André, J. M.; Kirtman, B. *J. Chem. Soc., Faraday Trans.* **1995**, *91*, 1641. (c) Champagne, B.; Vanderhoeven, H.; Perpète, E. A.; André, J. M. *Chem. Phys. Lett.* **1996**, *248*, 301. (d) Champagne, B. *Chem. Phys. Lett.* **1996**, *261*, 57. (e) Kirtman, B.; Champagne, B.; André, J. M. *J. Chem. Phys.* **1996**, *104*, 4125. (f) Kirtman, B.; Champagne, B. *Int. Rev. Phys. Chem.* **1997**, *16*, 389.

(10) (a) Cammi, R.; Cossi, M.; Tomasi, J. *J. Chem. Phys.* **1996**, *104*, 4611. (b) Cammi, R.; Cossi, M.; Mennucci, B.; Tomasi, J. *J. Chem. Phys.* **1996**, *105*, 10556.

(11) Mikkelsen, K. V.; Sylvester-Hvid, K. O. *J. Phys. Chem.* **1996**, *100*, 9116.

(12) Willets, A.; Rice, J. E. *J. Chem. Phys.* **1993**, *99*, 426.

(13) Wong, M. W.; Wiberg, K. B.; Frisch, M. J. *J. Chem. Phys.* **1991**, *95*, 8991.

(14) Mennucci, B.; Cammi, R.; Cossi, M.; Tomasi, J. *Theochem* **1998**, *426*, 191.

(15) Kanis, D. R.; Ratner, M. A.; Marks, T. J. *Chem. Rev.* **1994**, *94*, 195.

(16) Albert, I. D.; Marks, T. J.; Ratner, M. A. *J. Phys. Chem.* **1996**, *100*, 9714.

(17) (a) Marder, S. R.; Perry, J. W.; Temann, B. G.; Gorman, C. B.; Gilmour, S.; Biddle, S. L.; Bourhill, G. *J. Am. Chem. Soc.* **1993**, *115*, 2524. (b) Meyers, F.; Marder, S. R.; Pierce, B. M.; Bredas, J. L. *J. Am. Chem. Soc.* **1994**, *116*, 10703. (c) Marder, S. R.; Gorman, C. B.; Meyers, F.; Perry, J. W.; Bourhill, G.; Bredas, J. L.; Pierce, B. M. *Science* **1991**, *265*, 632.

distribution, leading thus to large effects on electronic and vibrational terms of linear and nonlinear optical properties.<sup>17</sup> As a consequence, although calculations on isolated molecules are helpful, a really important new step in the calculation of these properties is to explicitly take into account the influence of the medium surrounding the chromophore.

Previous studies in this direction have been performed by Albert et al.,<sup>16</sup> even with the limits of a partial analysis done only on the electronic terms of NLO properties, with a rather approximated solvent model and at a semiempirical level of calculation, and more recently by Gao and Alhambra<sup>18</sup> who have developed a hybrid quantum mechanical and molecular mechanical (QM/MM) technique to study solvent effects on BLA and absorption energy of conjugated compounds through Monte Carlo (MC) simulations. Another attempt to take into account the influence of the medium surrounding the NLO molecule has been done by Meyers et al.<sup>19</sup> Actually, their analysis is rather different from the previous ones, as they do not explicitly consider solvent effects but introduce an external electric field to qualitatively simulate these effects on nuclear geometry, electronic structure, and finally electronic optical properties.

A more detailed and complete step beyond gas-phase calculation is taken in the present work where we examine the influence of a continuum dielectric on both structure and electric response functions (dipole, static polarizability,  $\alpha$ , and first hyperpolarizability,  $\beta$ , both in their electronic and vibrational contributions) on chromophores such as linear polyenes. In particular, for the treatment of solvent effects we shall adopt the recent reformulation, known as integral equation formalism (IEF),<sup>20–22</sup> of the polarizable continuum method (PCM) developed in Pisa.<sup>23–25</sup>

The theoretical methodology is outlined in section 2, while in section 3 we present and discuss our calculation on two series of noncentrosymmetric polyenes of the type  $\text{NH}_2(\text{CH}=\text{CH})_n\text{R}$  ( $n = 1, 2$ ), that with  $\text{R} = \text{CHO}$  (series I) and the other with  $\text{R} = \text{NO}_2$  (series II).

## 2. Methodology and Computational Procedure

As already stated in the Introduction the properties which govern the response of a molecular system to an external applied electric field are the electronic and vibrational (hyper)polarizabilities. In the present paper we shall limit ourselves to analyze the static case only, but generalizations to frequency-dependent fields are rather immediate as we shall show in future papers now in progress.

For the calculation of the electronic quantities, there are two conceptually different approaches: the sum-over-states (SOS) and the derivative methods.

The SOS method is based on the perturbation expansion of the Stark energy. Different-order Stark energy terms are related to optical nonlinearities on the basis of their order in the field strength. The result is expressions for the polarizability and hyperpolarizabilities as infinite sums over various excited states in which the numerators contain dipole and transition dipole moments between couples of states.

The second method, here indicated as the derivative method, which constitutes the theoretical tool beyond the numerical

(18) Gao, J.; Alhambra, C. *J. Am. Chem. Soc.* **1997**, *119*, 2962.

(19) Reference 17b.

(20) Cancès, E.; Mennucci, B. *J. Math. Chem.*, in press.

(21) Cancès, E.; Mennucci, B.; Tomasi, J. *J. Chem. Phys.* **1997**, *107*, 3031.

(22) Mennucci, B.; Cancès, E.; Tomasi, J. *J. Phys. Chem. B* **1997**, *101*, 10506.

(23) Miertuš, S.; Scrocco, E.; Tomasi, J. *J. Chem. Phys.* **1981**, *55*, 117.

(24) Tomasi, J.; Persico, M. *Chem. Rev.* **1994**, *94*, 2027.

(25) Cammi, R.; Tomasi, J. *J. Comput. Chem.* **1995**, *16*, 1449.

results presented below, involves quantum calculations of energy or dipole moment followed by obtaining derivatives either numerically or analytically. The analytical approach for the derivative method involves mathematical relations widely known as generalized coupled perturbed Hartree–Fock (CPHF) equations, which are derived from the variational properties of the molecular wave function.

A term which represents the interaction between the external electric field and the instantaneous molecular dipole is added to the ordinary Hartree–Fock one-electron potential. The related HF equation is then expanded as a power series in this field, of magnitude  $F$ , and solved self-consistently order by order. In this way field-induced electron reorganization effects are taken into account. Finally each (hyper)polarizability is obtained by calculating the appropriate term in the expression for the induced dipole moment:

$$\mu_r = \mu_r^0 + \sum_s \alpha_{rs}^e F_s + (1/2!) \sum_{st} \beta_{rst}^e F_s F_t + \dots \quad (1)$$

where the index 0 refers to the molecular permanent dipole;  $\alpha^e$  and  $\beta^e$  are the electronic polarizability and first hyperpolarizability tensors, respectively, while the subscripts  $r, s, t, \dots$  refer to the Cartesian components of the external field.

It is immediate to see that, for a one-determinant wave function expanded over a finite basis set, when the CPHF equations are solved, i.e., the first ( $\mathbf{P}^s$ ) and second derivatives ( $\mathbf{P}^{st}$ ) of the density matrix with respect to the field are computed, the electronic (hyper)polarizabilities tensor components are given by<sup>26,27</sup>

$$\begin{aligned} \alpha_{rs}^e &= -tr[\mathbf{m}_r \mathbf{P}^s] \\ \beta_{rst}^e &= -tr[\mathbf{m}_r \mathbf{P}^{st}] \end{aligned} \quad (2)$$

where  $\mathbf{m}_r$  collects the integrals of the  $r$ th Cartesian component of the dipole moment operator.

Recently a PCM implementation allowing the computation of electronic (hyper)polarizabilities in both the static and frequency-dependent<sup>10</sup> cases has been proposed; in this framework, use is made of the CPHF and time-dependent coupled Hartree–Fock (TDCHF) formulations, respectively. The formal aspects of the implementation can be found in the source papers;<sup>10</sup> here it is sufficient to recall that, to obtain analytical derivatives, one has to substitute the Stark energy of the procedure in vacuo with the free energy functional,  $G$ , of the whole solute–solvent system:

$$\begin{aligned} G &= tr\mathbf{P}\mathbf{h} + (1/2)tr\mathbf{P}(\mathbf{j} + \mathbf{y}) + (1/2)tr\mathbf{P}[\mathbf{G}(\mathbf{P}) + \mathbf{X}(\mathbf{P})] + \\ &\quad (1/2)U_{\text{NN}} + V_{\text{NN}} \\ &= tr\tilde{\mathbf{P}}\tilde{\mathbf{h}} + (1/2)tr\tilde{\mathbf{P}}\tilde{\mathbf{G}}(\mathbf{P}) + V_{\text{NN}} \end{aligned} \quad (3)$$

Here the tilde stresses that the related matrices contain terms accounting for the presence of the solvent field through the matrices  $\mathbf{j}$ ,  $\mathbf{y}$ , and  $\mathbf{X}(\mathbf{P})$ .  $\tilde{V}_{\text{NN}}$  in eq 3 is a scalar term collecting nuclear repulsion ( $V_{\text{NN}}$ ) and the interaction ( $U_{\text{NN}}$ ) between solute nuclear charges and the solvent field they generate. Details on the physical and numerical bases underlying the method can be found in the already quoted papers.

In the following we shall also report results obtained from the random-phase approximation (RPA) method which is formally equivalent to the CPHF procedure, both in vacuo and

in solvent, but at the same time allows a SOS-like analysis of the relative contributions of the various excited states to electronic response functions. For more details on the equivalence between CPHF and RPA results when solvent effects are taken into account within the IEF-PCM model, see ref 28.

In the same way that there are two major techniques for calculation of the electronic (hyper)polarizabilities, so there are for the vibrational components (or better for their nuclear relaxation contributions,  $\alpha^{\text{nr}}$ , and  $\beta^{\text{nr}}$ ): the perturbation-theory and the finite field approximation.

As for the electronic case, also here the application of perturbation theory produces a sum-over-states expression for the components of the vibrational (hyper)polarizability tensors (from now on we shall skip the index nr from the relaxation components, and indicate them simply as vibrational terms):<sup>29,30</sup>

$$\alpha_{rs}^{\text{v}} = [\mu^2]$$

$$\beta_{rst}^{\text{v}} = [\mu\alpha] + [\mu^3] \quad (4)$$

where once again the subscripts  $r, s, t, \dots$  correspond to the Cartesian molecular axes. The square bracket quantities represent sums over vibrational states of quotients in which the numerator is a product of vibrational transition moments of electronic properties and the denominator contains vibrational frequencies, for example

$$[\mu^2] = \sum_k \frac{\langle 0|\mu_r|k\rangle\langle k|\mu_s|0\rangle}{E_k} \quad (5)$$

where  $|k\rangle$  is the  $k$ th vibrational wave function with energy  $E_k$  relative to the ground state whose vibrational wave function is  $|0\rangle$ . The sum excludes the vibrational ground state.

There are various ways in which the vibrational transition moments and energies can be determined. Here we shall focus on the method, developed by Bishop and Kirtman,<sup>29,30</sup> in which the electronic properties ( $M = \mu, \alpha^e, \dots$ ) are expressed in a power series in the normal coordinates ( $Q_a, Q_b, \dots$ ):

$$M_r = M_r^0 + \sum_a \left( \frac{\partial M_r}{\partial Q_a} \right)_0 Q_a + \frac{1}{2} \sum_{ab} \left( \frac{\partial^2 M_r}{\partial Q_a \partial Q_b} \right)_0 Q_a Q_b + \dots \quad (6)$$

where quadratic (and higher) order terms account for electrical anharmonicity.

Similarly, the vibrational potential is expanded as

$$V = V^0 + (1/2) \sum_a \omega_a^2 Q_a^2 + (1/6) \sum_{abc} f_{abc} Q_a Q_b Q_c + \dots \quad (7)$$

with the cubic and higher-order terms being the source of mechanical anharmonicity.

Within this framework the square-bracketed components of eq 4 can be subdivided according to order in anharmonicity; this is usually indicated by superscripts  $n$  and  $m$ , i.e.,  $[\ ]^{(n,m)}$ , where  $n$  is the order of electrical and  $m$  of mechanical anharmonicity. When only  $[\ ]^{(0,0)}$  terms are included, we have the double-harmonic approximation (only electric first and mechanical second derivatives with respect to  $Q$  are present) and

(26) Sekino, H.; Bartlett, R. J. *J. Chem. Phys.* **1986**, *85*, 976.

(27) Karna, S. P.; Dupuis, M. *J. Comput. Chem.* **1991**, *12*, 487.

(28) Cammi, R.; Mennucci, B. Submitted for publication.

(29) Bishop, D. M.; Kirtman, B. *J. Chem. Phys.* **1991**, *95*, 2646.

(30) Bishop, D. M.; Kirtman, B. *J. Chem. Phys.* **1992**, *97*, 5255.

$$\beta_{rst}^v = [\mu\alpha]^{(0,0)} \quad (8)$$

since no double-harmonic terms exist for  $[\mu^3]$ .

In this approximation, by defining each vibrational state by the quantum numbers associated with each of the  $3N - 6$  normal modes of the system, the final expressions of the vibrational contributions to the electric (hyper)polarizability tensor components become (in au)

$$\alpha_{rs}^v = \sum_a^{3N-6} \left( \frac{\partial \mu_r}{\partial Q_a} \right)_0 \left( \frac{\partial \mu_s}{\partial Q_a} \right)_0 / \omega_a^2 \quad (9)$$

$$\beta_{rst}^v = \sum_a^{3N-6} \left[ \left( \frac{\partial \mu_t}{\partial Q_a} \right)_0 \left( \frac{\partial \alpha_{rs}^e}{\partial Q_a} \right)_0 + \left( \frac{\partial \mu_s}{\partial Q_a} \right)_0 \left( \frac{\partial \alpha_{rt}^e}{\partial Q_a} \right)_0 + \left( \frac{\partial \mu_r}{\partial Q_a} \right)_0 \left( \frac{\partial \alpha_{st}^e}{\partial Q_a} \right)_0 \right] / \omega_a^2 \quad (10)$$

where  $\omega_a = 2\pi\nu_a$  is the circular frequency associated with  $Q_a$  and each partial derivative is evaluated at the equilibrium geometry.

To show the validity of the double harmonic procedure described above when the solvent interactions are taken into account within the IEF-PCM framework, it becomes compulsory to do a brief digression on the formal derivation of eqs 9 and 10.

As already stressed in the previous analysis on electronic (hyper)polarizabilities, also here the basic theoretical point which distinguishes in vacuo from solution calculations, is the introduction of the free energy functional  $G$ , see eq 3, which becomes the equivalent of the potential  $V$  energy reported in eq 7 when solute–solvent interactions are taken into account.<sup>31</sup> As a final result, this leads to substituting all the quantities in eqs 9 and 10 with the values obtained from the solvation calculation; in this scheme both the electric properties (dipole and polarizabilities) and the circular frequency have to be computed as derivatives of  $G$  with respect to the field and the normal coordinates, respectively. In addition the latter are adjusted to be correct for the solvated system. For brevity's sake we prefer to postpone the whole formal derivation of the formula above, well-known for the isolated system but much less theoretically stated for the solute, until the end of the paper, in Appendix 1. Here we limit ourselves to stress some important points.

Both eqs 9 and 10 require the computations of various electric and energy quantities. At the beginning of the section we have recalled that IEF-PCM manages to evaluate electronic properties by applying the equivalent of the CPHF scheme for the solvated system; moreover it can compute analytical gradient of the free energy with respect to nuclear coordinates, and consequently it is always possible to optimize the solute geometry in the presence of the solvent.<sup>32</sup> Regarding the latter point it is worth recalling that the geometry optimization of PCM molecular solutes is now particularly efficient thanks to the new procedure introduced in the IEF-PCM scheme to obtain solute–solvent interaction energy gradients.<sup>33</sup> The latter are here also exploited

to numerically compute the Hessian matrix and then to evaluate the frequencies  $\omega_a$ . In this way we can compute both electronic and vibrational (hyper)polarizabilities taking into account all the possible effects due to the presence of the continuum dielectric on the solute geometry, its electronic charge distribution, and the vibrational motions of its nuclei.

As a different but still important preliminary note, we recall that all the results reported below are obtained by assuming an implicit approximation in the model, namely, that the solvent reaction field is always equilibrated to that of the solute, also during its vibrational motions; the latter assumption should require some further comments; for brevity's sake we prefer not to report them here, but to refer the interested reader to the already quoted review, as containing some original observations on the subject,<sup>24</sup> and to two more specific papers.<sup>34</sup>

Before passing to the second, alternative procedure, a last important point needs to be considered in treating systems in solutions, namely, the problem of local field effects. All the relations derived above are analytically exact if the external applied field can be considered uniform; actually this external, macroscopic electric field is altered by its passage through the medium, and this change is reflected by the incorporation of “local field factors” into the relation between the macroscopic and the microscopic field really acting on the local position of the molecule:

$$\vec{E}_{\text{loc}} = \mathbf{f}\vec{E}$$

where  $\mathbf{f}$  is a  $3 \times 3$  tensor whose components are the “local-field factors”.

In determining the local field one must, in general, take into account the depolarizing field acting on any particular molecule due to the influence of the surrounding molecules. This is a quite challenging task which has received the attention of theoreticians over many decades, although analytical results are available in only a few simple cases. Very recently, two new techniques have been presented, one analytical,<sup>35</sup> as generalization of the Onsager reaction field, and the other numerical.<sup>36</sup> The latter constitutes a simple but effective procedure to compute  $\mathbf{f}$  for molecular solutes of general shape in the IEF framework, in order to analyze the implications this additional solvent effect has on the electronic static (hyper)polarizabilities of various molecular solutes. A parallel analysis should surely be done for the vibrational contributions too. In the present paper we only limit to stress the existence of this problem, not considering its numerical effects; their detailed treatment will be the subject of a future communication.

An alternative method to calculate vibrational (hyper)polarizabilities, above indicated as finite field approximation, has been recently developed by Bishop et al.<sup>37</sup> This method requires no direct knowledge of the electronic-property derivatives, force constants, etc. All that is replaced by a set of much simpler finite-field calculations with and without allowing nuclei to relax to equilibrium position when an external static electric field  $F$  is present.

If we denote the equilibrium molecular geometry with a static electric field present by  $R_F$  and without the field by  $R_0$ , then for any electronic property  $M$  we may define

(34) (a) Olivares del Valle, F. J.; Tomasi, J. *J. Chem. Phys.* **1987**, *114*, 231. (b) Aguilar, M. A.; Olivares del Valle, F. J. *J. Chem. Phys.* **1990**, *150*, 151.

(35) Wortmann, R.; Bishop, D. M. *J. Chem. Phys.* **1998**, *108*, 1001.

(36) Cammi, R.; Mennucci, B.; Tomasi, J. *J. Phys. Chem. A* **1998**, *102*, 870.

(37) Bishop, D. M.; Hasan, M.; Kirtman, B. *J. Chem. Phys.* **1995**, *103*, 4157.

(31) Tomasi, J.; Mennucci, B.; Cammi, R.; Cossi, M. In *Quantum mechanical models for reactions in solution in Computational Approaches to Biochemical Reactivity*; Naray-Szabo, G., Warshel, A., Eds.; Kluwer Academic Publishers: Dordrecht, 1997; Vol. 19, pp 1–102.

(32) Cammi, R.; Tomasi, J. *J. Chem. Phys.* **1994**, *101*, 3888.

(33) (a) Cancès, E.; Mennucci, B. *J. Chem. Phys.* **1998**, *109*, 229. (b) Cancès, E.; Mennucci, B.; Tomasi, J. *J. Chem. Phys.* **1998**, *109*, 260.

$$(\Delta M)_{R_0} = M(F, R_0) - M(0, R_0) \quad (11)$$

and

$$(\Delta M)_{R_F} = M(F, R_F) - M(0, R_0) \quad (12)$$

For small  $F$ , both of these quantities may be fitted to a Taylor expansion in the field.

In particular, when  $M = \mu$ , eq 11 is reduced to eq 1 reported above for the electronic contribution to the (hyper)polarizabilities, while eq 12 becomes (see also eq 24) of Appendix 1)

$$(\Delta \mu_r)_{R_F} = \sum_s a_1(r, s) F_s + (1/2!) \sum_{st} b_1(r, s, t) F_s F_t + \dots \quad (13)$$

The coefficients here are intrinsically different from those of eq 1. They now contain the vibrational contribution due to relaxation of the molecular geometry caused by the applied static field. These contributions are those previously called the nuclear relaxation components of the vibrational (hyper)polarizabilities. It is easy to see that

$$\begin{aligned} a_1(r, s) &= \alpha_{rs}^v + \alpha_{rs}^e \\ b_1(r, s, t) &= \beta_{rst}^v + \beta_{rst}^e \end{aligned} \quad (14)$$

where once again the superscript  $v$  indicates only the relaxation part of the vibrational contribution. Once the coefficient in eq 13 have been obtained by finite field fitting techniques, the relaxation component of the static vibrational (hyper)polarizabilities can be found from eq 14, together with the known static electronic values.

The vibrational quantities obtained in this way include the lowest-order nonvanishing perturbation terms of each type that appear in the Bishop–Kirtman treatment reported above. In particular we have

$$\begin{aligned} \alpha_{rs}^v &= [\mu^2]^{(0,0)} \\ \beta_{rst}^v &= [\mu\alpha]^{(0,0)} + [\mu^3]^{(1,0)} + [\mu^3]^{(0,1)} \end{aligned} \quad (15)$$

where we have exploited the already used formalism indicating the various anharmonicities.

To make a more reliable comparison between quantities obtained within the finite-field procedure and those derived from the double harmonic approximation of the perturbative method (see eqs 9 and 10), it is worth considering a further application of eq 12, this time in terms of the electronic polarizability tensor  $\alpha^e$ . By limiting the related Taylor expansion to the first order in the field, we can write

$$(\Delta \alpha_{rs}^e)_{R_F} = \sum_t b_2(r, s, t) F_t + \dots \quad (16)$$

with

$$b_2(r, s, t) = \beta_{rst}^v(-\omega; \omega, 0)_{\omega \rightarrow \infty} + \beta_{rst}^e \quad (17)$$

The subscript  $\omega \rightarrow \infty$  denotes that the vibrational term is obtained in the “infinite frequency” limit, which means that any fields used to determine  $\alpha_{rs}^e$  in the left-hand side of eq 16 are distinct from the structure-changing field  $F$  and can be considered to oscillate with infinite frequency, so that they cannot affect molecular geometries. It may be noted that the same type of contribution that appears in the static equivalents

appears in the infinite frequency approximation but with different numerical factors (including zero); in particular for the diagonal term  $\beta_{rrr}^v$  we have

$$\beta_{rrr}^v(-\omega; \omega, 0)_{\omega \rightarrow \infty} = (1/3)[\mu\alpha]_{\text{static}}^{(0,0)} \quad (18)$$

From eq 18 it immediately follows that the right quantity to be compared with the double-harmonic value of the vibrational first hyperpolarizability of eq 10 is the infinite frequency  $\beta_{rst}^v(-\omega; \omega, 0)_{\omega \rightarrow \infty}$  and not the static one deriving from eq 14, as the latter contains further contributions from both electric and mechanical anharmonicity (see eq 15).

More details on this point will be analyzed in the numerical section, where we shall report numerical results for the full set of quantities presented above.

As a final note we recall that the introduction of the solvent effects within this scheme does not lead to any basic changes; the whole procedure remains valid if all the electric properties,  $\mu$ ,  $\alpha^e$ , and  $\beta^e$ , as well as both the zero-field and the field-relaxed solute geometries are computed in the presence of the reaction field due to the continuum dielectric.

### 3. Numerical Results and Discussion

In this section we shall present and discuss some numerical results regarding static electronic and vibrational (hyper)polarizabilities of two series of noncentrosymmetric polyenes:  $\text{NH}_2(\text{CH}=\text{CH})_n\text{R}$  ( $n = 1, 2$ ), with  $\text{R} = \text{CHO}$  (series I) and with  $\text{R} = \text{NO}_2$  (series II). As the molecules are taken to lie in the  $xy$ -plane (actually the exact planarity is lost in solution) with the long axis oriented along the  $x$ -axis, the dominant components are  $\alpha_{xx}$  for the polarizability, and  $\beta_{xxx}$  for the first hyperpolarizability; in the following our analysis will be limited to these diagonal components only.

All the calculations have been performed at the SCF level with a basis set equal to the Dunning/Huzinaga valence double- $\zeta^{38}$  as given by Gaussian94 code.<sup>40</sup> The choice of basis set in the calculation of (hyper)polarizabilities is quite a delicate point. It is in fact well known that these quantities require extended basis sets including polarization and diffuse functions; to justify our choice of a rather limited basis set, we remark that we are here mainly interested in the analysis of relative quantities and of general trends rather than in the evaluation of the best (hyper)polarizability values. As a matter of fact previous calculations<sup>39</sup> on series II have shown that the CPHF calculation with the use of a quite small basis (in that work 6-31G) underestimates both dipole and first hyperpolarizability (nothing is reported for the polarizability) as compared to results with extra diffuse functions, but it reproduces the  $\mu$ -value to 98% of that for 6-31G+1p1d, and the large part of the  $\beta$ -diagonal value. In addition it has been seen that the basis set effect generally becomes small with the increase of molecular size; hence, for the two largest components of both series, the eventual error due to the limited BS is even less important.

All the calculations in solution have been performed using the IEF version of the PCM method. Within this framework,

(38) Dunning, T. H., Jr.; Hay, P. J. In *Modern Theoretical Chemistry*; Schaefer, H. F., III, Ed.; Plenum: New York, 1976; pp 1–28.

(39) Tsunekawa, T.; Yamaguchi, K. *J. Phys. Chem.* **1992**, *96*, 10268.

(40) Frisch, M. J.; Trucks, G. W.; Schlegel, H. B.; Gill, P. M. W.; Johnson, B. G.; Robb, M. A.; Cheeseman, J. R.; Keith, T.; Petersson, G. A.; Montgomery, J. A.; Raghavachari, K.; Al-Laham, M. A.; Zakrzewski, V. G.; Ortiz, J. V.; Foresman, J. B.; Peng, C. Y.; Ayala, P. Y.; Chen, W.; Wong, M. W.; Andres, J. L.; Replogle, E. S.; Gomperts, R.; Martin, R. L.; Fox, D. J.; Binkley, J. S.; Defrees, D. J.; Baker, J.; Stewart, J. P.; Head-Gordon, M.; Gonzalez, C.; Pople, J. A. *Gaussian 94*, Revision D.4; Gaussian, Inc.: Pittsburgh, PA, 1995.

**Table 1.** Static Electronic and Vibrational (Hyper)polarizabilities (au) of  $\text{H}_2\text{N}(\text{CH}=\text{CH})_n\text{R}$  (with  $\text{R} = \text{CHO}, \text{NO}_2$  and  $n = 1, 2$ ) in vacuo<sup>a</sup>

	CHO		NO <sub>2</sub>	
	$n = 1$	$n = 2$	$n = 1$	$n = 2$
$\alpha_{rr}^e$	70.57	140.51	71.32	146.73
$\alpha_{rr}^v$	21.32	39.81	21.09	43.90
$\alpha_{rr}^{ev}$	91.89	180.32	92.41	190.63
$\beta_{rrr}^e$	-398.7	-1437.6	-490.4	-1893.7
$\beta_{rrr}^v$	-642.0	-2489.1	-922.6	-3846.7
$\beta_{rrr}^{ev}$	-1040.7	-3926.7	-1413.0	-5740.4

<sup>a</sup> Electronic components are obtained from CPHF procedures, while vibrational terms are computed from eqs 9 and 10 of the text.

**Table 2.** Static Electronic and Vibrational (Hyper)polarizabilities (au) of  $\text{H}_2\text{N}(\text{CH}=\text{CH})_n\text{R}$  (with  $\text{R} = \text{CHO}, \text{NO}_2$  and  $n = 1, 2$ ) in Water<sup>a</sup>

	CHO		NO <sub>2</sub>	
	$n = 1$	$n = 2$	$n = 1$	$n = 2$
$\alpha_{rr}^e$	103.03	231.23	122.04	319.43
$\alpha_{rr}^v$	60.67	174.81	123.87	1003.44
$\alpha_{rr}^{ev}$	163.70	406.04	245.91	1322.87
$\beta_{rrr}^e$	-899.9	-4701.3	-1227.2	-1928.4
$\beta_{rrr}^v$	-2259.3	-17125.2	-5458.0	-12675.5
$\beta_{rrr}^{ev}$	-3159.2	-21826.5	-6685.2	-14603.9

<sup>a</sup> Electronic components are obtained from CPHF procedures, while vibrational terms are computed from eqs 9 and 10 of the text.

the molecular solute is embedded in a cavity in the dielectric medium defined in terms of interlocking spheres centered on the solute nuclei, with radii  $R_k$  equal to 1.2 times the corresponding van der Waals values  $R_k^{\text{vdw}}$ ; namely, for our solutes we have  $R_{\text{H}} = 1.44 \text{ \AA}$ ,  $R_{\text{C}} = 2.04 \text{ \AA}$ ,  $R_{\text{O}} = 1.80 \text{ \AA}$ , and  $R_{\text{N}} = 1.92 \text{ \AA}$ . The solvation calculations are performed for a medium having dielectric constant  $\epsilon = 78.5$  corresponding to the static dielectric constants of liquid water at 298 K.

All the geometry optimizations, both in vacuo and in solution, with and without applied external field, have been performed by exploiting the G94 code, where IEF analytical gradients have been recently implemented.<sup>33</sup> On the contrary, all the electronic properties,  $\alpha^e$  and  $\beta^e$ , and the vibrational ones (in the approximation of double harmonicity, see eqs 9 and 10) are computed with GAMESS code,<sup>41</sup> in which the IEF-PCM version of CPHF procedure has also been implemented.<sup>22</sup>

Regarding the geometry optimization with applied external fields, we also add that the exploited algorithm is the Berny algorithm using redundant internal coordinates which eliminates the rotational degrees of freedom, no longer free, and consequently automatically solves the problem of possible reorientation of the molecule due to the external field (this problem has been stressed in many studies; see, e.g., Martí et al.<sup>42</sup>). Numerical evidence of this statement will be given below.

In Tables 1 and 2 we report the results obtained for the static electronic and vibrational (in the double harmonic approximation) polarizability and hyperpolarizability for the two series of molecules both in vacuo and in solution.

(41) Schmidt, M. W.; Baldridge, K. K.; Boatz, J. A.; Elbert, S. T.; Gordon, M. S.; Jensen, J. H.; Koseki, S.; Matsunaga, N.; Nguyen, K. A.; Su, S. J.; Windus, T. L.; Dupuis, M.; Montgomery, J. A. *J. Comput. Chem.* **1993**, *14*, 1347.

(42) Martí, J.; Andrés, J. L.; Bertrán, J.; Duran M. *Mol. Phys.* **1993**, *80*, 625.

**Table 3.** Bond Lengths (Å) of  $\text{H}_2\text{N}(\text{CH}=\text{CH})\text{R}$  in Vacuo and in Water<sup>a</sup>

	CHO		NO <sub>2</sub>	
	vacuum	water	vacuum	water
$R_{\text{XY}}$	1.2284	1.2506	1.2478	1.2696
$R_{\text{CX}}$	1.4543	1.4304	1.4216	1.3721
$R_{\text{CC}}$	1.3511	1.3696	1.3494	1.3809
$R_{\text{CN}}$	1.3664	1.3448	1.3552	1.3236

<sup>a</sup> If  $\text{R} = \text{CHO}$ ,  $\text{X} = \text{C}$  and  $\text{Y} = \text{O}$ ; otherwise, when  $\text{R} = \text{NO}_2$ ,  $\text{X} = \text{N}$  and  $\text{Y} = \text{O}$ .

**Table 4.** Bond Lengths (Å) of  $\text{H}_2\text{N}(\text{C}_4\text{H}=\text{C}_3\text{HC}_2\text{H}=\text{C}_1\text{H})\text{R}$  in Vacuo and in Water<sup>a</sup>

	CHO		NO <sub>2</sub>	
	vacuum	water	vacuum	water
$R_{\text{XY}}$	1.2274	1.2477	1.2464	1.2830
$R_{\text{C}_1\text{X}}$	1.4608	1.4385	1.4311	1.3540
$R_{\text{C}_1\text{C}_2}$	1.3483	1.3645	1.3440	1.3949
$R_{\text{C}_2\text{C}_3}$	1.4507	1.4329	1.4413	1.3896
$R_{\text{C}_3\text{C}_4}$	1.3499	1.3661	1.3550	1.3966
$R_{\text{CN}}$	1.3728	1.3526	1.3644	1.3229

<sup>a</sup> If  $\text{R} = \text{CHO}$ ,  $\text{X} = \text{C}$  and  $\text{Y} = \text{O}$ ; otherwise, when  $\text{R} = \text{NO}_2$ ,  $\text{X} = \text{N}$  and  $\text{Y} = \text{O}$ .

**Table 5.** Bond Length Alternation (BLA) (Å) of  $\text{H}_2\text{N}(\text{CH}=\text{CH})_2\text{R}$  in Vacuo and in Water

	vacuum	water
CHO	0.1067	0.0704
NO <sub>2</sub>	0.0917	-0.00614

To make our analysis clearer, the discussion on the results reported in Tables 1 and 2 will be divided into three parts, focused on geometry effects, electronic (hyper)polarizability terms, and vibrational components.

**3.1. Geometry Effects.** As reported in the Introduction, the extent of geometric distortions induced by solvent or an external electric field can be characterized by bond length alternation (BLA), defined as the average difference in length between single and double bonds in the conjugated pathway (it is by convention taken as positive in the neutral polyene-like form).

In Tables 3 and 4 we report the bond lengths of the first element of both series at the geometries optimized in vacuo and in solution, while in Table 5 the BLA values for the second terms of each series of molecules (for the first terms it is not possible to define a BLA as the conjugated path is limited).

The two main aspects to be pointed out are the effects due to the nature of substituents and, more important, to the presence of the solvent.

From both Tables 3 and 4 it results that more polar D–A substituents (i.e., molecules of series II) act to reduce the length of the single bonds and to increase the length of the double bonds. The same effect, even if largely amplified, is given by the presence of the solvent; in the latter case the BLA decreases from 0.1067 to 0.0704 for  $\text{NH}_2(\text{CH}=\text{CH})_2\text{CHO}$ , and from +0.0917 to -0.0061 for  $\text{NH}_2(\text{CH}=\text{CH})_2\text{NO}_2$ , passing from gas phase to aqueous solution.

This large solvent effect on equilibrium geometries is in good accord with the results obtained by Gao and Alhambra,<sup>18</sup> even if in this work a completely different model is used to represent the solvent molecules (i.e., MC simulations) and a QM/MM level of calculation is performed. In this paper, limited to series I (for the second term they use the doubly substituted  $\text{N}(\text{CH}_3)_2$  as donor group), the authors find, for the first term, a decrease of the single CC bond length on the order of 0.023 Å and an

**Table 6.** Ground-State Dipole Moment (D) and Mulliken Net Charges (au) of R-(X1=X2-X3=X4)-NH<sub>2</sub> (with R = CHO, NO<sub>2</sub>) Both in Gas Phase and in Aqueous Solution

	$\mu_r$	group charges (au)					NH <sub>2</sub>
		R	X1	X2	X3	X4	
CHO <sub>(g)</sub>	-6.3179	-0.1555	-0.0531	+0.2699			-0.0612
CHO <sub>(aq)</sub>	-9.2531	-0.2602	-0.1131	+0.3475			+0.0258
CHO <sub>(g)</sub>	-7.7909	-0.1605	-0.0571	+0.1037	-0.0381	+0.2339	-0.0820
CHO <sub>(aq)</sub>	-12.0932	-0.2599	-0.1253	+0.1769	-0.0935	+0.3047	-0.0029
NO <sub>2(g)</sub>	-8.1474	-0.4420	+0.0705	+0.3925			-0.0211
NO <sub>2(aq)</sub>	-12.3971	-0.6449	+0.0684	+0.4582			+0.1183
NO <sub>2(g)</sub>	-10.1829	-0.4492	+0.0514	+0.2323	-0.0569	+0.2815	-0.0590
NO <sub>2(aq)</sub>	-19.6363	-0.7548	+0.0296	+0.2807	-0.0656	+0.4059	+0.1041

increase of the double bond length of 0.021 Å (to be compared with 0.024 and 0.019 Å of our calculations), while for the second term a decrease of 0.036 Å in the BLA value (exactly equal to our value). On the contrary, in the other related paper on solvent effects by Albert et al.,<sup>16</sup> the change in geometry of the similar (CH<sub>3</sub>)<sub>2</sub>N(CH=CH)<sub>4</sub>CHO molecule passing from vacuum to water is much less important; the computed decrease of BLA is only 0.012 Å. As the authors themselves observe, this small solvent effect is maybe due to the use of a spherical cavity, which for such extended solutes is clearly inadequate, and also to the truncation of the multipole expansion describing the solute charge distribution at the dipole term. These two evident limitations are completely absent in our model where a molecular-shaped cavity is used and a full description of the solute charge distribution, without any approximation, is exploited.

For completeness' sake, we add that many other data obtained for similar D-A polyenes both experimentally, see for example ref 17a, and theoretically, see Cho<sup>43</sup> for a very recent study, can further confirm our results of an evident reduction of the BLA due to the presence of the polar solvent.

In addition, data reported in Table 5 clearly show that, as one might expect, the presence of a polar solvent like water induces a migration of electronic charge distribution along the molecular axis from the D to A group; in this way the electronic structure of the molecular system, which in the gas phase is well characterized by a polyene-like structure only, in solution contains a large contribution also from the partially charge-separated cyanine-like form: in NH<sub>2</sub>(CH=CH)<sub>2</sub>NO<sub>2</sub> in water the BLA becomes almost zero, exactly as in an ideal cyanine structure.

The same conclusions can be reached in a different way, by taking into account the changes on the net charges of the various chemical groups present in the molecule, when passing from gas phase to solution. In Table 6 we report the total dipole moment and the Mulliken net charges on the D-A groups as well as on the intermediate CH groups both in vacuo and in solution.

The most evident result of data reported in Table 6 is that the A group, which in vacuo shows significant partial negative charges in both series, in solution presents a positive charge, with the only exception of the second term of series I where the A net charge is almost zero. This behavior once again shows that in solution the cyanine-like structure assumes a much more important role and becomes the main one for series II. The electron migration toward the A group is reflected also in the net charges of the intermediate CH groups which all increase in magnitude passing from vacuum to aqueous solution.

(43) Cho, M. *J. Phys. Chem. A* **1998**, *102*, 703. For a coherent comparison with our results it is worth noting that, in this paper, the author, following a previous related paper by Kim, H.-S.; Cho, M.; Jeon, S.-J. *J. Chem. Phys.* **1997**, *107*, 1936, adopts a convention on the sign of the BLA parameter opposite ours, i.e., negative values for the neutral canonical resonance form.

**Table 7.** Percent Variations of Electronic and Vibrational Contributions of Static (Hyper)polarizabilities of H<sub>2</sub>N(CH=CH)<sub>n</sub>R Passing from the Gas Phase to the Aqueous Solution:  $\Delta M = 100[M(\text{aq}) - M(\text{gas})]/M(\text{gas})$ 

	CHO		NO <sub>2</sub>	
	<i>n</i> = 1	<i>n</i> = 2	<i>n</i> = 1	<i>n</i> = 2
$\delta\alpha_{rr}^e$	+46	+64	+71	+118
$\delta\alpha_{rr}^v$	+185	+339	+487	+2186
$\delta\beta_{rrr}^e$	+126	+227	+150	+2
$\delta\beta_{rrr}^v$	+152	+588	+492	+230

**Table 8.** Dipole Variations (D) with Respect to the Ground-State Value,  $\Delta\mu_r^{\text{gn}}$ , Transition Energies (eV),  $\Delta E^{\text{gn}}$ , and Oscillatory Strength (au), *f*, for the Lowest Allowed Single Excitation of H<sub>2</sub>N(CH=CH)<sub>n</sub>R Molecules Both in Gas Phase and in Aqueous Solution

	<i>f</i>	$\Delta\mu_r^{\text{gn}}$	$\Delta E^{\text{gn}}$
CHO(1) <sub>(g)</sub>	0.784	-2.017	6.280
CHO(1) <sub>(aq)</sub>	0.989	-1.366	5.369
CHO(2) <sub>(g)</sub>	1.283	-3.446	5.257
CHO(2) <sub>(aq)</sub>	1.523	-2.522	4.154
NO <sub>2</sub> (1) <sub>(g)</sub>	0.445	-4.040	5.593
NO <sub>2</sub> (1) <sub>(aq)</sub>	0.725	-2.331	4.364
NO <sub>2</sub> (2) <sub>(g)</sub>	0.967	-5.448	4.834
NO <sub>2</sub> (2) <sub>(aq)</sub>	1.284	-0.859	3.287

**3.2. Electronic (Hyper)polarizabilities.** The larger mobility of the electronic charge in the presence of the solvent we have derived from the analysis on geometrical changes of the previous subsection is also made evident by the significant increase in the electronic polarizability passing from gas phase to solution. This is shown in Table 7 in which we report the percent variation of electronic and vibrational polarizability and first hyperpolarizability of both series of molecules.

Limiting our attention to the electronic data of Table 7 (the vibrational part will be analyzed in the next subsection), we can also observe another interesting solvent effect, maybe less predictable. The first hyperpolarizability  $\beta^e$  which, in both terms of the series I, presents significant increments going from gas phase to solution (from 126% to 227%), in series II shows an unexpected behavior with a very small increase in the solvated NH<sub>2</sub>(CH=CH)<sub>2</sub>NO<sub>2</sub> molecule; here  $\beta^e$  is only 2% larger than the vacuum result. This result, which is completely different from those of the other computed molecules and also from the usual values reported in the literature for other push-pull systems,<sup>44,45</sup> needs a more detailed analysis. To do that, in Table 8 we report the RPA results of the lowest allowed single excitation from the GS for all the molecules both in vacuo and in solution.

(44) Mikkelsen, K. V.; Luo, Y.; Ågren, H.; Jørgensen, P. *J. Chem. Phys.* **1994**, *100*, 8240.

(45) Di Bella, S.; Marks, T. J.; Ratner, M. A. *J. Am. Chem. Soc.* **1994**, *116*, 4440.

**Table 9.** Static Electronic Polarizability and First Polarizability (au) in the Two-Level Model for  $\text{H}_2\text{N}(\text{CH}=\text{CH})_n\text{R}$  Both in the Gas Phase and in Aqueous Solution<sup>a</sup>

	$\alpha_{rr}^e$	$\beta_{rrr}^e$
CHO(1) <sub>(g)</sub>	39.22 (55.6)	-269.7 (67.6)
CHO(1) <sub>(aq)</sub>	69.98 (67.9)	-381.2 (42.4)
CHO(2) <sub>(g)</sub>	94.03 (66.9)	-1319.8 (91.8)
CHO(2) <sub>(aq)</sub>	182.2 (78.8)	-2368.6 (50.4)
NO <sub>2</sub> (1) <sub>(g)</sub>	31.47 (44.1)	-487.0 (99.0)
NO <sub>2</sub> (1) <sub>(aq)</sub>	84.26 (69.0)	-964.3 (78.6)
NO <sub>2</sub> (2) <sub>(g)</sub>	91.38 (62.3)	-2206.5 (116.5)
NO <sub>2</sub> (2) <sub>(aq)</sub>	263.48 (82.5)	-1475.2 (76.5)

<sup>a</sup> Values in parentheses refer to the percentage of the property with respect to its CPHF total value.

As already reported in the previous section on methodology, the RPA procedure, even if formally equivalent to CPHF, allows one to perform an analysis of the electronic (hyper)polarizabilities in terms of sums of contributions from different electronic excited states (SOS). A very simple scheme which is very useful for interpretative purposes, even if not reliable from a quantitative point of view, limits the SOS expression to a unique excited state. In the resulting two-state approximation (TSA), the static diagonal electronic polarizability and first hyperpolarizability are given by

$$\alpha_{rr}^e = 2 \frac{(\mu_r^{\text{gn}})^2}{\Delta E^{\text{gn}}} = 3 \frac{f^{\text{gn}}}{(\Delta E^{\text{gn}})^2} \quad (19)$$

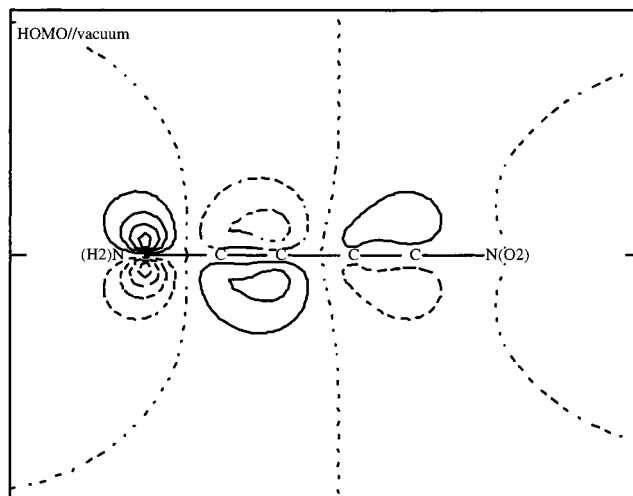
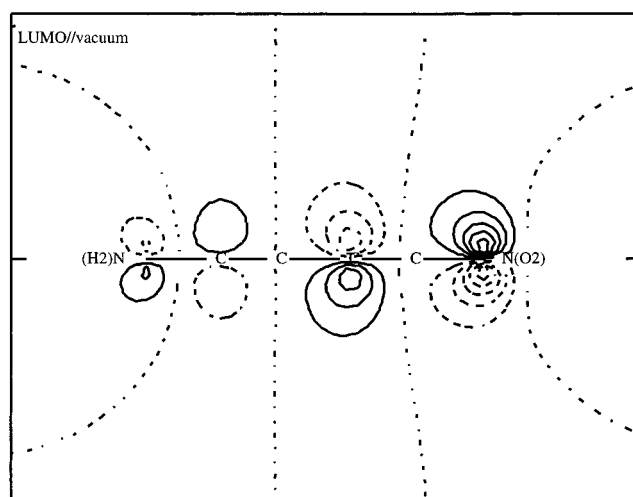
$$\beta_{rrr}^e = 4 \frac{(\mu_r^{\text{gn}})^2 \Delta \mu_r^{\text{gn}}}{(\Delta E^{\text{gn}})^2} = 6 \frac{f^{\text{gn}} \Delta \mu_r^{\text{gn}}}{(\Delta E^{\text{gn}})^3} = 2 \frac{\alpha_{rr}^e \Delta \mu_r^{\text{gn}}}{\Delta E^{\text{gn}}} \quad (20)$$

where  $\mu_r^{\text{gn}}$  is the  $r$  component of the dipole transition moment between the ground and excited states,  $\Delta E^{\text{gn}}$  is the corresponding excitation energy,  $\Delta \mu_r^{\text{gn}}$  is the change in the  $r$  component of the dipole moment between the ground and excited states, and  $f^{\text{gn}} = 2\mu_r^{\text{gn}2} \Delta E^{\text{gn}}/3$  is the oscillatory strength (in the equations above we have assumed that the transition dipole moment is completely described by its  $r$  component, i.e.,  $\mu_r^{\text{gn}} \approx (\mu^{\text{gn}})^2$ ).

In Table 9 we report the static (hyper)polarizability values obtained both in vacuo and in solution by applying eqs 19 and 20.

The main point to be stressed is that the TSA only gives qualitative results; the very small discrepancies between TSA and analytical  $\alpha^e$  and  $\beta^e$  values found for some molecules are almost fortuitous; in one case TSA even overestimates the analytical  $\beta^e$ . Anyway, TSA establishes an important link between electronic properties and spectroscopic quantities.

A quite evident result derivable from data of Table 9 is that the important increase of the polarizability in solution is largely due to the red shift of the transition energy; in both the series the  $\delta \Delta E^{\text{gn}}$  is around 1 eV ( $\sim 8000 \text{ cm}^{-1}$ ). This bathochromic shift, which has also been experimentally observed in similar push–pull systems,<sup>46</sup> corresponds to a situation where, through the interaction with the solvent reaction field, the first excited state is preferentially stabilized with respect to the GS being its dipole moment larger than that in the GS. Once again, due to the strong link present in these  $\pi$ -conjugated systems between geometry and electronic structure, the same conclusions can be reached from considerations on BLA changes: the red shift in the transition can take place as the GS in solution becomes described by equal contributions from the polyene form and

**Figure 2.**  $xz$  plane contour map of HOMO for  $\text{NH}_2(\text{CH}=\text{CH})_2\text{NO}_2$  in vacuo.**Figure 3.**  $xz$  plane contour map of LUMO for  $\text{NH}_2(\text{CH}=\text{CH})_2\text{NO}_2$  in vacuo.

the partially charge-separated form, i.e., the cyanine limit (and in fact the largest shift,  $\delta \Delta E^{\text{gn}} = 1.54 \text{ eV}$ , is given by  $\text{NH}_2(\text{CH}=\text{CH})_2\text{NO}_2$  for which a very small BLA is also found).

In the RPA-SOS framework also the unusual behavior found for the  $\beta^e$  of  $\text{NH}_2(\text{CH}=\text{CH})_2\text{NO}_2$  in solution assumes a clearer meaning. From Table 8, it is evident that the most irregular data regarding this molecule is the very small change in the transition dipole moment from the GS to the first allowed excited state in solution with respect to the parallel value in vacuo ( $-0.859 \text{ D}$  vs  $-5.448 \text{ D}$ ); due to the proportionality of  $\beta^e$  and  $\Delta \mu_r^{\text{gn}}$ , the final result is the observed small increase of the first hyperpolarizability of the solvated molecular system with respect to the value computed in vacuo. On the contrary, this kind of behavior is not shown by the polarizability which is not related to  $\Delta \mu_r^{\text{gn}}$ ; as a matter of fact,  $\alpha^e$  presents a standard large increase also for  $\text{NH}_2(\text{CH}=\text{CH})_2\text{NO}_2$ .

To better understand this phenomenon, we recall that the excited state can be almost exclusively described by one basic excitation (typically highest occupied molecular orbital (HOMO)  $\rightarrow$  lowest unoccupied molecular orbital (LUMO)); for the same reason the TSA is often referred to as the two-level approximation. In this picture it is interesting to report in Figures 2–5 the plot of the two involved molecular orbitals both in vacuo and in solution (for all the molecules analyzed in the present paper the HOMO–LUMO transition is a  $\pi \rightarrow \pi^*$  transition).

(46) Reichardt, C. *Solvents and Solvent Effects in Organic Chemistry*; VCH: Weinheim, 1990.

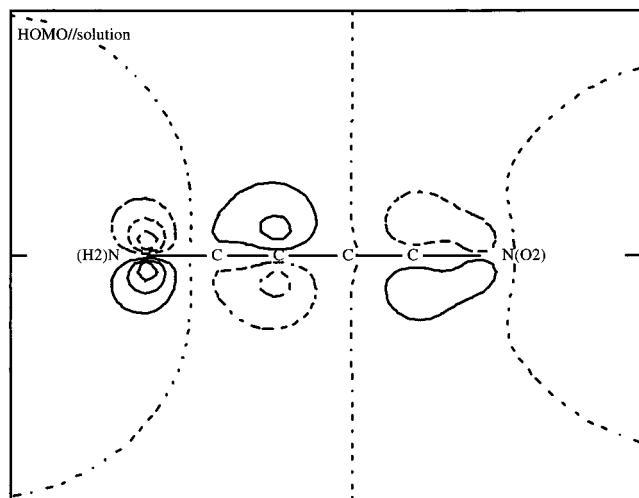


**Figure 4.** *xz* plane contour map of HOMO for  $\text{NH}_2(\text{CH}=\text{CH})_2\text{NO}_2$  in solution.

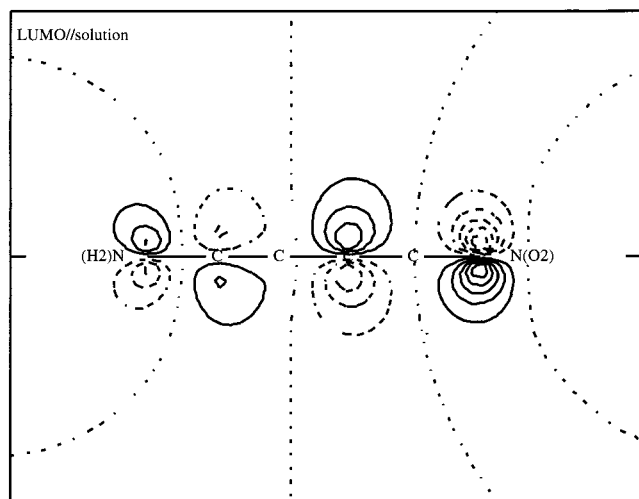


**Figure 5.** *xz* plane contour map of LUMO for  $\text{NH}_2(\text{CH}=\text{CH})_2\text{NO}_2$  in solution.

From Figures 2 and 4 we can see that the general form of the HOMO does not change too much from gas phase to solution, and in fact the coefficients of the two MOs relative to the atomic functions centered on the two N atoms of the D–A groups are very similar ( $q_{\text{N}_\text{D}} = \sum_i c_i^2(\text{N}_\text{D})$  is 0.178 au in vacuo and 0.111 au in solution, whereas  $q_{\text{N}_\text{A}} = \sum_i c_i^2(\text{N}_\text{A})$  is 0.000 au in vacuo and 0.024 au in solution). Things are not so similar for the LUMO; Figures 3 and 5 present in fact a rather different aspect relatively to the N of the amine group whose  $q_{\text{N}_\text{D}}$  value goes from 0.070 au in vacuo to 0.116 au in solution. This means that in the charge-transfer excitation HOMO–LUMO, the variation of the  $q_{\text{N}_\text{D}}$  is  $-0.108$  au in vacuo and almost zero in water (the parallel value of  $\delta_{\text{N}_\text{A}}$  is 0.253 au in vacuo and 0.269 au in solution); consequently, the dipole moment change passing from the GS to the excited state, which in vacuo presents a large value, is very small in solution, as small is the increase of  $\beta^e$ .

**3.3. Vibrational Hyperpolarizabilities.** Going back to Tables 1 and 2, what remains to be analyzed is the vibrational component of hyperpolarizabilities, and the effects the solvent induces on this quantity. Before beginning the discussion on results it is worth recalling that the vibrational term we shall consider here contains the nuclear relaxation term only; as already stressed in the Introduction the curvature term due to the field-induced changes in the potential energy surface and

**Table 10.** Ratios between Vibrational and Electronic (Hyper)polarizabilities of  $\text{H}_2\text{N}(\text{CH}=\text{CH})_n\text{R}$  in Gas Phase and in Aqueous Solution

	CHO				NO <sub>2</sub>			
	<i>n</i> = 1		<i>n</i> = 2		<i>n</i> = 1		<i>n</i> = 2	
	gas	aq	gas	aq	gas	aq	gas	aq
$\alpha_{rr}^v/\alpha_{rr}^e$	0.302	0.589	0.283	0.756	0.296	1.015	0.299	3.145
$\beta_{rrr}^v/\beta_{rrr}^e$	1.610	2.511	1.731	3.643	1.881	4.448	2.031	6.573

including zero-point vibrational correction (ZPC), will not be considered in the present paper.

As a first element of analysis, in Table 10 we report the ratios between vibrational and electronic (hyper)polarizabilities both in vacuo and in solution for all the molecules of the two series presented in the previous subsections.

Regarding static polarizabilities, previous calculations on other conjugated systems in vacuo<sup>47</sup> have given  $\alpha^v/\alpha^e$  ratios ranging from 0.1 to 0.4; in Table 10 a value of about 0.3 is computed for all four molecules in vacuo. On the contrary, no comparisons with data from the literature can be made for solvated systems, as never studied before. Anyway, the results of Table 10 when combined with those of Table 2 show that the solvent effects induce either a large increase in the absolute vibrational contribution and, even more evident, a net larger increase of the latter with respect to the electronic component; in series II the ratio  $\alpha^v/\alpha^e$  in solution is greater than 1, and the vibrational component becomes dominant.

A similar analysis can be done on the first hyperpolarizability; also here vacuum results are in good accord with previous calculations on conjugated systems; for example, for  $\text{NH}_2(\text{CHCH})_2\text{NO}_2$  Kirtman and Champagne find a ratio of 2.20 with a RHF/6-31G calculation<sup>48</sup> to be compared with 2.03 of Table 10. Once more, solvent effects lead to large increases in the relative importance of the vibrational contribution with respect to the electronic one multiplying the gas phase value of  $\beta^v/\beta^e$  by factors from 1.5 (in the first term of series I) to 2 (in the second term of series II).

Once the most evident aspects of the computed numerical results have been so pointed out, the further step to be done is their analysis. To do that, it is worth going back to eqs 9 and 10 giving the formal relations between (hyper)polarizabilities and normal modes of the molecule. As we have done in the TSA approximation of electronic contributions where we have defined a single excited state able to give a reliable description of the (hyper)polarizabilities, also here we can hope to find a single mode  $Q^*$  (corresponding to frequency  $\omega^*$ ) which plays the most important role in the determination of  $\alpha^v$  and  $\beta^v$ .

Actually, the analysis on normal modes is not as easy as those on electronic states, and unfortunately it is not possible to find a single mode which could reproduce the full vibrational property at a good qualitative level; two or more modes have then to be considered.

In Table 11 we report the frequency, the IR intensity, and the relative contribution to  $\alpha^v$  and  $\beta^v$  obtained in the double harmonic approximation for the two modes which contribute most to vibrational (hyper)polarizabilities of the molecules of series I both in vacuo and in solution.

What results from the data of Table 11 is that for the first molecule in vacuo the two main modes globally reproduce 40% of total  $\alpha^v$  and 62% of  $\beta^v$ ; the remaining is partitioned among many other modes with contributions  $\leq 5\%$ . In solution, besides

(47) Reference 9b,c.

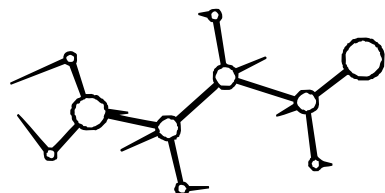
(48) Reference 9f.

**Table 11.** Spectroscopic and (Hyper)polarizability Contributions of the Two Main Normal Modes for Series I ( $\text{NH}_2(\text{CH}=\text{CH})_n\text{CHO}$ , with  $n = 1, 2$ ) Both in Vacuo and in Solutions<sup>a</sup>

	freq	IR	$\alpha_{rr}^v$	$\beta_{rrr}^v$
Mode 1				
$n = 1_{(g)}$	1840.63	21.08069	6.85 (32)	-301.83 (47)
$n = 1_{(aq)}$	1723.97	53.81693	18.95 (31)	-1001.4 (44)
$n = 2_{(g)}$	1825.65	33.23892	10.61 (27)	-1355.1 (54)
$n = 2_{(aq)}$	1676.11	116.20251	44.00 (25)	-5498.1 (32)
Mode 2				
$n = 1_{(g)}$	1277.99	2.51939	1.69 (8)	-97.5 (15)
$n = 1_{(aq)}$	1284.37	21.48950	14.83 (24)	-629.7 (25)
$n = 2_{(g)}$	1297.46	4.73956	3.21 (8)	-450.3 (18)
$n = 2_{(aq)}$	1228.77	88.04280	65.01 (37)	-7175.4 (42)

<sup>a</sup> Frequencies are in  $\text{cm}^{-1}$ , IR intensities in  $\text{D}^2/(\text{amu} \text{ \AA}^2)$ . Values in parentheses refer to the percentage of the contribution with respect to the double-harmonic vibrational value reported in Tables 1 and 2.

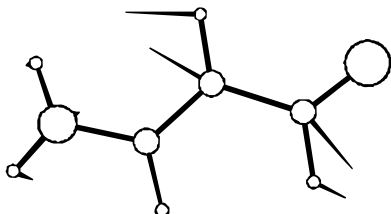
R=CHO//N=1



MODE 1//vacuum

**Figure 6.** Drawing of normal mode 1 of  $\text{NH}_2(\text{CH}=\text{CH})\text{CHO}$  in vacuo.

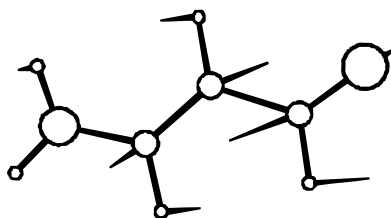
R=CHO//N=1



MODE 2//vacuum

**Figure 7.** Drawing of normal mode 2 of  $\text{NH}_2(\text{CH}=\text{CH})\text{CHO}$  in vacuo.

R=CHO//N=1



MODE 1//solution

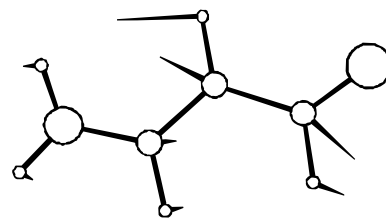
**Figure 8.** Drawing of normal mode 1 of  $\text{NH}_2(\text{CH}=\text{CH})\text{CHO}$  in solution.

the two equivalents of modes 1 and 2 in vacuo which now globally give 55% of  $\alpha^v$  and 69% of  $\beta^v$ , there appears another rather important mode of very low frequency ( $591.57 \text{ cm}^{-1}$ ), not reported in Table 11, contributing 8% of  $\alpha^v$  and 13% of  $\beta^v$ .

Modes 1 and 2, both in vacuo and in solution, contain a main component related to  $\text{C}=\text{C}$  and  $\text{C}-\text{C}$  stretching of the chain, respectively. This is shown in Figures 6–9, in which we plot the drawings of the two modes in mass-weighted Cartesian coordinates.

The changes induced by the solvent are evident on both frequencies and IR intensities; what we observe is a significant decrease of frequency ( $\sim 117 \text{ cm}^{-1}$ ) and an important increase

R=CHO//N=1



MODE 2//solution

**Figure 9.** Drawing of normal mode 2 of  $\text{NH}_2(\text{CH}=\text{CH})\text{CHO}$  in solution.

in IR intensity (by a factor of 2.5) for mode 1, and, for mode 2, a small increase of frequency ( $\sim 6 \text{ cm}^{-1}$ ) accompanied by a very large increase in IR intensity (by a factor of 8.5). Let us try to analyze these data in a more detailed way, as they can give useful information for a more physical description of  $\alpha^v$  and  $\beta^v$ . The direct relation between polarizability and spectroscopic data is explicitly shown in eq 9 if we recall that IR intensity is proportional to  $(\partial\mu/\partial Q)^2$ ; the parallel relation for  $\beta^v$  is a little more complex as it also involves Raman intensities, but for our scope we can limit our consideration to the still present proportionality between  $\beta^v$  and  $\partial\mu/\partial Q$ , and then IR intensities.

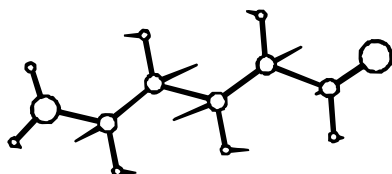
In a very qualitative picture, the observed behaviors can be related to the changes in the CC bond lengths reported in Table 3 as well as to the transfer of electronic charge from the donor to the acceptor group shown in Table 6. As in solution we observe a lengthening of the double bond and a parallel shortening of the single CC bond, it is well acceptable that the frequencies will be smaller for mode 1 and larger for mode 2, the two modes related to  $\text{C}=\text{C}$  and  $\text{C}-\text{C}$  stretching, respectively. On the other hand, as the additional motion associated with the main  $\text{C}=\text{C}$  stretching in mode 1 involves different groups passing from vacuo to solution, namely,  $\text{NH}_2$  and  $\text{CHO}$ , the IR intensity, as well as the contributions to  $\alpha^v$  and  $\beta^v$ , in solution will be larger as larger is the dipole variation related to distortions of  $\text{CHO}$  in solution than of  $\text{NH}_2$  in vacuo.

For mode 2, in which the groups involved remain almost equivalent in vacuo and in solution, the large amplification of IR intensity (and consequently of the contribution of this mode to (hyper)polarizabilities) passing to the solvated system is clearly related to effects of electron transfer toward  $\text{CHO}$ . In fact, as the main distortion characteristic of this mode,  $\text{C}-\text{C}$  stretching, involves the C atom of the  $\text{CHO}$  group, the related dipole variations and IR intensity will be largely amplified in solution.

A parallel analysis can be done on the second term of the same series. Also in this case two are the main modes which globally give 35% of  $\alpha^v$  and 72% of  $\beta^v$  in vacuo, and 62% of  $\alpha^v$  and 74% of  $\beta^v$  in solution. However, for this larger molecule, the almost complete equivalence found before for both modes in vacuo and in solution does not appear any more, or better it is not fulfilled in mode 2. Mode 1 is not changed too much passing from the gas phase to solution; only the related frequency is decreased  $\sim 150 \text{ cm}^{-1}$  for the same reason, inducing the parallel decrease observed for mode 1 in the previous molecule. The drawings of the two modes, both in vacuo and in solution, are reported in Figures 10–13.

As can be seen from Figures 11 and 13, mode 2 in vacuo mainly involves a stretching of the central single  $\text{C}-\text{C}$  bond, while in solution this stretching is shifted on the terminal  $\text{C}-\text{C}(\text{HO})$  bond, with also a small contribution from the first  $\text{C}=\text{C}$  bond contraction. Once again, this change can be

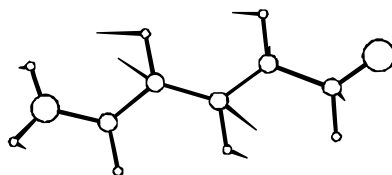
R=CHO/N=2



MODE 1//vacuum

**Figure 10.** Drawing of normal mode 1 of  $\text{NH}_2(\text{CH}=\text{CH})_2\text{CHO}$  in vacuo.

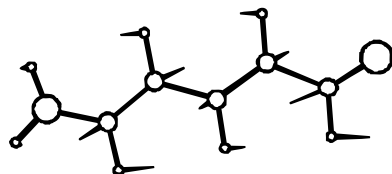
R=CHO/N=2



MODE 2//vacuum

**Figure 11.** Drawing of normal mode 2 of  $\text{NH}_2(\text{CH}=\text{CH})_2\text{CHO}$  in vacuo.

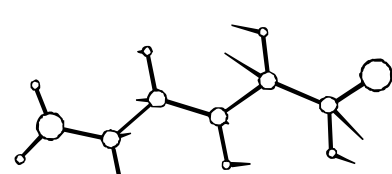
R=CHO/N=2



MODE 1//solution

**Figure 12.** Drawing of normal mode 1 of  $\text{NH}_2(\text{CH}=\text{CH})_2\text{CHO}$  in solution.

R=CHO/N=2



MODE 2//solution

**Figure 13.** Drawing of normal mode 2 of  $\text{NH}_2(\text{CH}=\text{CH})_2\text{CHO}$  in solution.

explained in terms of the important changes induced by the solvent on the bond lengths and on the related BLA reported in Tables 4 and 5, as well as on the electronic charge distribution shown in Table 6. In solution, in fact, the CC bond pattern partially loses the clear structure characteristic of the system in vacuo, and differences between single and double bonds become less evident. As a consequence the motions of the various CC groups can be changed and/or mixed together to give different resulting normal modes. In addition, the great effects that CHO distortions can induce on dipole derivatives in solution lead to a migration of the effective motions toward the acceptor group and to an IR intensity which is larger by a factor of  $\sim 19$  with respect to that of mode 2 in vacuo.

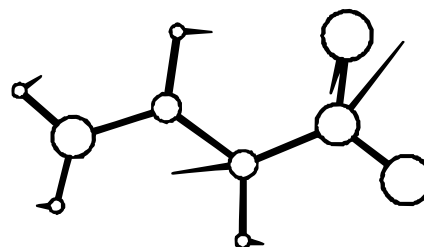
The parallel analysis on the other group of molecules (series II) is complicated by various elements; first the number of normal modes which contribute in a significant way increases by at least one, and second, the whole description loses the clear correspondence between gas phase and solution results found for the previous series. In this series in fact, the solvent effects on geometry, i.e., BLA, and electronic charge distribution are

**Table 12.** Spectroscopic and (Hyper)polarizability Contributions of the Main Normal Mode for Series II ( $\text{NH}_2(\text{CH}=\text{CH})_n\text{NO}_2$ , with  $n = 1, 2$ ) Both in Vacuo and in Solutions<sup>a</sup>

	mode 1			
	freq	IR	$\alpha_{rr}^v$	$\beta_{rrr}^v$
$n = 1_{(g)}$	1406.18	3.97176	6.03 (29)	-485.1 (53)
$n = 1_{(aq)}$	1168.09	82.17219	68.92 (56)	-2920.2 (54)
$n = 2_{(g)}$	1366.06	25.47721	14.87 (34)	-1275.0 (33)
$n = 2_{(aq)}$	863.93	279.33417	424.01 (42)	-6408.3 (51)

<sup>a</sup> Frequencies are in  $\text{cm}^{-1}$ , IR intensities in  $\text{D}^2/(\text{amu} \text{ \AA}^2)$ . Values in parentheses refer to the percentage of the contribution with respect to the double-harmonic vibrational value reported in Tables 1 and 2.

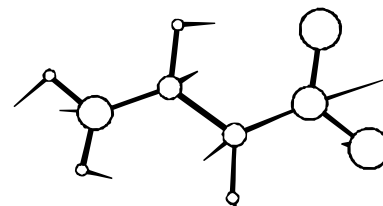
R=NO2/N=1



MODE 1//vacuum

**Figure 14.** Drawing of normal mode 1 of  $\text{NH}_2(\text{CH}=\text{CH})\text{NO}_2$  in vacuo.

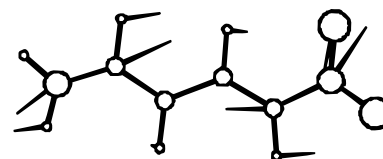
R=NO2/N=1



MODE 1//solution

**Figure 15.** Drawing of normal mode 1 of  $\text{NH}_2(\text{CH}=\text{CH})\text{NO}_2$  in solution.

R=NO2/N=2



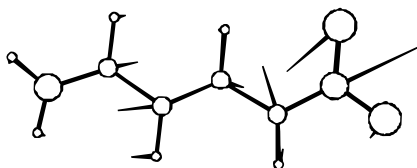
MODE 1//vacuum

**Figure 16.** Drawing of normal mode 1 of  $\text{NH}_2(\text{CH}=\text{CH})_2\text{NO}_2$  in vacuo.

so large that the relative importance of the various modes in terms of  $\alpha^v$  and  $\beta^v$  contributions completely changes passing from the gas phase to solution. From a different point of view, we can say that what was observed as a secondary effect in the first series, i.e., structural differences between vacuum and solution modes which increase in the larger term of the series, is here so amplified to become the key aspect. Let us try to better understand this point by limiting our analysis to the mode giving the most important contribution of  $\alpha^v$  and  $\beta^v$ .

In Table 12 we report frequency, IR intensity, and (hyper)polarizability contributions of this main mode for each term of the series both in vacuo and in solution, and in Figures 14–17 we plot the related drawings.

In the smaller molecule, the correspondence of the modes for gas phase and solvated systems is still present, and both mainly involve a  $\text{C}-\text{N}(\text{O}_2)$  stretching; the only important changes to be stressed are on the frequency which decreases

R=NO<sub>2</sub>/N=2

MODE 1/solution

**Figure 17.** Drawing of normal mode 1 of NH<sub>2</sub>(CH=CH)<sub>2</sub>NO<sub>2</sub> in solution.**Table 13.** Taylor Coefficients of Eq 14 for NH<sub>2</sub>(CHCH)CHO in Vacuo with Respect to Applied External Field  $F$  (au)<sup>a</sup>

$F$	$a_1$	$[\mu\alpha]^{(0,0)}$	$b_1$	
			I	II
0.0016	93.12	-701.7	-1137.1	-1131.7
0.0008	93.08	-688.1	-1102.3	-1090.7
0.0004	93.08	-688.6	-855.6	-773.4

<sup>a</sup>  $b_1$  is given in terms of the two formulas shown in eq 23;  $[\mu\alpha]^{(0,0)}$  is obtained from the  $b_2$  coefficient of eq 16 through eqs 17 and 18.**Table 14.** Taylor Coefficients of Eq 14 for NH<sub>2</sub>(CHCH)CHO in Water with Respect to Applied External Field  $F$  (au)<sup>a</sup>

$F$	$a_1$	$[\mu\alpha]^{(0,0)}$	$b_1$	
			I	II
0.0016	165.61	-2276.1	-4457.3	-4458.7
0.0008	165.65	-2310.9	-4204.2	-4119.8
0.0004	165.80	-2298.0	-3490.6	-3656.8

<sup>a</sup>  $b_1$  is given in terms of the two formulas shown in eq 23;  $[\mu\alpha]^{(0,0)}$  is obtained from the  $b_2$  coefficient of eq 16 through eqs 17 and 18.

~240 cm<sup>-1</sup>, and on IR intensity which on the contrary increases by a factor of ~20 passing from vacuum to solution. This large solvent effect is again strongly related to changes in C–N(O<sub>2</sub>) bond length (for which we obtain a decrease of 0.033 Å in solution) and to the charge transfer from the donor to the acceptor which leads to large dipole derivatives, and hence large IR intensities and  $\alpha^v$  and  $\beta^v$  contributions, when distortion of the NO<sub>2</sub> group is possible.

The latter effect is particularly evident in the second molecule of the series. Here the stretching/contraction motions of the conjugated chain which typically contribute most to vibrational (hyper)polarizabilities of these molecules, as we have seen in the other series, are substituted by other modes passing from gas phase to solution. As a result, the new main mode of the solvated system becomes strongly related to internal distortions of the NO<sub>2</sub> group, and the frequency goes from 1400 cm<sup>-1</sup> in gas phase to 864 cm<sup>-1</sup> in solution. This solvent-induced shifting of the effective motions toward the acceptor group is then further shown in the other two important modes (not reported in Table 12) giving globally 41% of  $\alpha^v$  and 62% of  $\beta^v$  (the sum of the main contributions to  $\beta^v$  can be larger than the final value as there are some modes which give terms of opposite signs) and showing very low frequencies, 650 and 690 cm<sup>-1</sup>, respectively. The two equivalent modes in gas phase, on the contrary, still show the typical pattern of conjugated chain systems dominated by CC double and single bond stretchings at frequencies of ~1800 and ~1300 cm<sup>-1</sup>, respectively.

**3.3.1. Finite Field Analysis.** As a last element of analysis we report in Tables 13–20 the results obtained by applying the finite field approximation expressed by eqs 11–18.

Before discussing the meaning of data reported in Tables 13–20, some technical considerations on the numerical procedure are required. As any finite difference technique, also that exploited here needs some preliminary checks to obtain stable

**Table 15.** Taylor Coefficients of Eq 14 for NH<sub>2</sub>(CHCH)<sub>2</sub>CHO in Vacuo with Respect to Applied External Field  $F$  (au)<sup>a</sup>

$F$	$a_1$	$[\mu\alpha]^{(0,0)}$	$b_1$	
			I	II
0.0016	182.27	-2643.0	-4538.1	-4517.6
0.0008	182.31	-2614.2	-4487.5	-4470.2
0.0004	182.27	-2611.5	-4088.1	-3995.1

<sup>a</sup>  $b_1$  is given in terms of the two formulas shown in eq 23;  $[\mu\alpha]^{(0,0)}$  is obtained from the  $b_2$  coefficient of eq 16 through eqs 17 and 18.**Table 16.** Taylor Coefficients of Eq 14 for NH<sub>2</sub>(CHCH)<sub>2</sub>CHO in Water with Respect to Applied External Field  $F$  (au)<sup>a</sup>

$F$	$a_1$	$[\mu\alpha]^{(0,0)}$	$b_1$	
			I	II
0.0016	412.49	-17236.1	-41515.9	-41444.6
0.0008	409.40	-17266.2	-38406.1	-37369.8
0.0004	408.82	-17206.8	-40276.9	-40900.5

<sup>a</sup>  $b_1$  is given in terms of the two formulas shown in eq 23;  $[\mu\alpha]^{(0,0)}$  is obtained from the  $b_2$  coefficient of eq 16 through eqs 17 and 18.**Table 17.** Taylor Coefficients of Eq 14 for NH<sub>2</sub>(CHCH)NO<sub>2</sub> in Vacuo with Respect to Applied External Field  $F$  (au)<sup>a</sup>

$F$	$a_1$	$[\mu\alpha]^{(0,0)}$	$b_1$	
			I	II
0.0016	92.83	-919.4	-1760.3	-1753.1
0.0008	92.79	-919.6	-1682.8	-1657.0
0.0004	92.55	-910.7	-1418.8	-1330.7

<sup>a</sup>  $b_1$  is given in terms of the two formulas shown in eq 23;  $[\mu\alpha]^{(0,0)}$  is obtained from the  $b_2$  coefficient of eq 16 through eqs 17 and 18.**Table 18.** Taylor Coefficients of Eq 14 for NH<sub>2</sub>(CHCH)NO<sub>2</sub> in Water with Respect to Applied External Field  $F$  (au)<sup>a</sup>

$F$	$a_1$	$[\mu\alpha]^{(0,0)}$	$b_1$	
			I	II
0.0016	247.08	-5112.3	-15621.1	-15924.2
0.0008	247.17	-5322.1	-15546.2	-15521.3
0.0004	246.46	-5335.9	-12863.1	-11968.7

<sup>a</sup>  $b_1$  is given in terms of the two formulas shown in eq 23;  $[\mu\alpha]^{(0,0)}$  is obtained from the  $b_2$  coefficient of eq 16 through eqs 17 and 18.

results; in particular, as we exploit geometry optimizations with external electric field, great importance is assumed by the choice of the external field amplitude and of the convergence threshold for the residual forces on the atoms after the optimization.<sup>49</sup> For the latter point we have found that a threshold of  $1.2 \times 10^{-4}$  au/bohr is a good compromise; by repeating the optimizations with tighter values we have in fact found very small variations, less than the uncertainty inherent in the numerical procedure (see Tables 19 and 20). Regarding the external field amplitude, we have explored a quite large range, from 0.0002 to 0.0128 au (1 au of electrical field =  $5.142 \times 10^{11}$  V m<sup>-1</sup>), but the more stable results have been found with fields of 0.0004–0.0016 au of amplitude; for this reason in the tables we report these values only.

A further aspect to be defined is the finite difference expression used to calculate the components of the Taylor coefficients reported in eqs 14 and 17; in particular for the first-order quantities  $a_1$  and  $b_2$ , we have

$$a_1 \approx (1/2F_r)[\mu_r(F_r, R_F) - \mu_r(-F_r, R_{-F})] \quad (21)$$

$$b_2 \approx (1/2F_r)[\alpha_{rr}^c(F_r, R_F) - \alpha_{rr}^c(-F_r, R_{-F})] \quad (22)$$

while for the second-order  $b_1$  two different relations have been

**Table 19.** Taylor Coefficients of Eq 14 for NH<sub>2</sub>(CHCH)NO<sub>2</sub> in Vacuo with Respect to Applied External Field  $F$  (au)<sup>a</sup>

$F$	$a_1$		$[\mu\alpha]^{(0,0)}$	$b_1$			
				(T1)		(T2)	
	T1	T2		I	II	I	II
0.0016	191.60	191.49	-3878.5	-7634.5	-7638.9	-7601.6	-7586.6
0.0008	191.22	191.76	-3861.6	-8265.6	-8476.0	-7686.6	-7714.9
0.0004	191.26	191.69	-3854.7	-10830.6	-11685.6	-7712.5	-7721.1

<sup>a</sup>  $b_1$  is given in terms of the two formulas shown in eq 23;  $[\mu\alpha]^{(0,0)}$  is obtained from the  $b_2$  coefficient of eq 16 through eqs 17 and 18. Each quantity has been computed with two different convergency criteria: that exploited in the previous calculations in which the threshold on the force is  $1.2 \times 10^{-4}$  au/bohr (au/radian) (T1) and a stricter one with a threshold of  $6 \times 10^{-5}$  (T2).

**Table 20.** Taylor Coefficients of Eq 14 for NH<sub>2</sub>(CHCH)NO<sub>2</sub> in Water with Respect to Applied External Field  $F$  (au)<sup>a</sup>

$F$	$a_1$		$[\mu\alpha]^{(0,0)}$	$b_1$			
				(T1)		(T2)	
	T1	T2		I	II	I	II
0.0016	1085.28	1084.31	-8099.7	-24254.4	-27023.0	-24680.5	-27104.8
0.0008	1237.91	1238.13	-10586.0	-35618.9	-39407.1	-35825.6	-39540.7
0.0004	1301.93	1300.10	-11742.7	-50660.6	-55674.5	-62908.7	-71936.5

<sup>a</sup>  $b_1$  is given in terms of the two formulas shown in eq 23;  $[\mu\alpha]^{(0,0)}$  is obtained from the  $b_2$  coefficient of eq 16 through eqs 17 and 18.  $a_1$  and  $b_1$  have been computed with two different convergency criteria: that exploited in the previous calculations in which the threshold on the force is  $1.2 \times 10^{-4}$  au/bohr (au/radian) (T1) and a stricter one with a threshold of  $6 \times 10^{-5}$  (T2).

tested

$$b_1 \approx [\mu_r(F_r, R_F) - 2\mu_r(0, R_0) + \mu_r(-F_x, R_{-F})]/F_r^2 \quad (\text{I})$$

$$b_1 \approx [16(\mu_r(F_r, R_F) + \mu_r(-F_x, R_{-F})) - \mu_r(2F_x, R_{2F}) - \mu_r(-2F_x, R_{-2F}) - 30\mu_r(0, R_0)]/12F_r^2 \quad (\text{II}) \quad (23)$$

where  $F$  and  $R_F$  represent the external applied field and the molecular geometry optimized in the presence of this field ( $R_0$  is the zero-field optimized geometry). Theoretically, we could assume that the five-point procedure indicated as expression II in eq 23 gives more accurate results with respect to the parallel one exploiting only three points (expression I); actually the numerical data reported in Tables 13–20 show that both procedures are strongly dependent on the amplitude of the field.

The latter observation introduces a fundamental point of these calculations: the reliability, and the physical meaning, of the comparison with previous results obtained in the double harmonic approximation as sums over normal mode components.

The first thing to be stressed is that for first-order quantities, i.e.,  $a_1$  and  $[\mu\alpha]_{\text{static}}^{(0,0)}$  as directly obtained from  $b_2$  by applying eqs 17 and 18, the accord with the equivalent properties of Tables 1 and 2, namely,  $\alpha^e + \alpha^v$  and  $\beta^v$ , is quite good both in vacuo and in solution. This confirms two important formal aspects.

First, it gives the proof quoted at the beginning of the numerical section on the nonexistence of the problem of a possible reorientation of the molecule during the optimization in the presence of the external field when an algorithm using redundant internal coordinates is exploited. Second, it numerically shows the complete equivalence between in vacuo and in solution double-harmonic approximations formally shown in Appendix 1. The latter point assumes a very important aspect as the results presented here are the first ever computed on molecular systems in the condensed phase.

For  $b_1$  things are more complex, and also the numerical results are less stable; this can be related to two different problems. First, as  $b_1$  is a second-order quantity, i.e., it represents the second derivative of the dipole moment with respect to the external applied field, the numerical accuracy of this value will

be surely less than for first-order quantities; in our opinion this point is enough to explain the instability of some results, especially those of the largest molecules in solution (last column in Table 20) for which the inherent accuracy of the method cannot be equivalent to the calculation in vacuo, at variation of the field amplitude.

The second problem, of formal nature, is given by the presence of anharmonic components, namely, those indicated as  $[\mu^3]^{(1,0)} + [\mu^3]^{(0,1)}$  in the expression of  $b_1$  given in eq 15. These two terms, related to electric and mechanical anharmonicity, respectively, are not easy to compute as they involve third derivatives of the dipole moment and second derivatives of the potential energy  $V$  or, equivalently, of the functional free energy  $G$  for the system in solution. In addition, no many numerical data are available from the literature; only some small- and medium-sized molecules in vacuo have been studied in a general perturbation approach which enables considerations of higher and higher orders on both the mechanical and electrical anharmonicities,<sup>29,50</sup> but surely no results have ever been given for systems in solution.

What results from data reported in Tables 13–20 is that the computed discrepancies between  $b_1$  and the sum of electronic and double-harmonic vibrational hyperpolarizabilities (row indicated as  $\beta^{\text{ev}}$  in Tables 1 and 2) are too big to be induced by only numerical inaccuracy, but surely have to be related to anharmonic terms, which for all the molecules studied in the present paper seem to be quite important, especially in solution where they can even duplicate the double-harmonic values. This additional aspect, which partially goes beyond the scope of the present paper, is surely of interest and we hope to have the chance to explore it in a more detailed way in the very near future.

**Acknowledgment.** Financial support by the Consiglio Nazionale delle Ricerche is acknowledged.

## Appendix 1

The Taylor expansion reported in eq 1 is done assuming what is called the canonical or clamped-nuclei (CN) approximation. The latter essentially allows the external field  $F$  to act first on

(50) Bishop, D. M.; Dalskov, E. K. *J. Chem. Phys.* **1996**, *104*, 1004.

the electronic motions and then on the vibrational degrees of freedom rather than simultaneously on both.<sup>51</sup> In this case in fact the same expansion should be written in the form

$$\mu_r(R_F) = \mu_r^0(R_0) + \sum_s (\alpha_{rs}^e + \alpha_{rs}^v) F_s + (1/2!) \sum_{st} (\beta_{rst}^e + \beta_{rst}^v) F_s F_t + \dots \quad (24)$$

where  $R_F$  denotes the equilibrium molecular geometry with a static electric field present and  $R_0$  the parallel one without the field. The coefficients of the expansion are easily obtained by applying the rules on partial derivatives; namely, we have

$$\alpha_{rs}^e = \left( \frac{\partial \mu_r}{\partial F_s} \right)_{R_0} \quad (25)$$

$$\alpha_{rs}^v = \sum_i^{3N} \left( \frac{\partial R_i}{\partial F_s} \right)_{R_0} \left( \frac{\partial \mu_r}{\partial R_i} \right)_{R_0} \quad (26)$$

and

$$\beta_{rst}^e = \left( \frac{\partial^2 \mu_r}{\partial F_s \partial F_t} \right)_{R_0} \quad (27)$$

$$\beta_{rst}^v = \sum_i^{3N} \left[ \left( \frac{\partial R_i}{\partial F_t} \right)_{R_0} \left( \frac{\partial \alpha_{rs}^e}{\partial R_i} \right)_{R_0} + \left( \frac{\partial R_i}{\partial F_s} \right)_{R_0} \left( \frac{\partial \alpha_{rt}^e}{\partial R_i} \right)_{R_0} + \left( \frac{\partial^2 R_i}{\partial F_s \partial F_t} \right)_{R_0} \left( \frac{\partial \mu_r}{\partial R_i} \right)_{R_0} \right] \quad (28)$$

Equations 25–27 give the pure electronic (hyper)polarizabilities (they are exactly equivalent to the expressions reported in eq 2), while eqs 26–28 report the nuclear relaxation contributions to the vibrational (hyper)polarizabilities.

In the presence of the solvent, the derivatives with respect to the geometry which compare in eqs 26–28 can be obtained by recalling that for a molecular solute treated within the IEF-PCM framework the equilibrium geometry corresponds to a minimum of the functional free energy  $G(\mathbf{R})$  introduced in eq 3; as already noted  $G(\mathbf{R})$  is the equivalent of the potential energy  $V$  of eq 7 when solute–solvent interactions are taken into account.

If we indicate with  $\mathbf{d}$  the displacement in the solute equilibrium geometry due to the external field ( $\mathbf{R}_F = \mathbf{R}_0 + \mathbf{d}$ ), then, in the approximation of mechanical harmonic for  $G(\mathbf{F}, \mathbf{R})$ ,  $\mathbf{d}$  satisfies the following relation (from now on we prefer to shift to a matrix form for the vectorial quantities, indicating them with a bold character):

$$\mathbf{g} + \mathbf{H}\mathbf{d} = 0 \quad \text{or} \quad \mathbf{d} = -\mathbf{H}^{-1}\mathbf{g} \quad (29)$$

where  $\mathbf{g}$  and  $\mathbf{H}$  are the gradient and the Hessian, both computed at  $\mathbf{R}_0$ , of the free energy functional in the presence of the field, respectively

$$g_i = \left( \frac{\partial G(\mathbf{F}, \mathbf{R})}{\partial R_i} \right)_{\mathbf{R}_0} \quad (30)$$

$$[H]_{ij} = \left( \frac{\partial^2 G(\mathbf{F}, \mathbf{R})}{\partial R_i \partial R_j} \right)_{\mathbf{R}_0} \quad (31)$$

By introducing the expansion of  $G$  with respect to the field

$$G(\mathbf{F}, \mathbf{R}) = G(0, \mathbf{R}) - \sum_s \mu_s F_s - (1/2) \sum_{st} \alpha_{st}^e F_s F_t + \dots \quad (32)$$

we may rewrite eqs 30 and 31 in terms of Taylor expansions:

$$g_i = - \sum_s \left( \frac{\partial \mu_s}{\partial R_i} \right)_{\mathbf{R}_0} F_s - \frac{1}{2} \sum_{st} \left( \frac{\alpha_{st}^e}{\partial R_i} \right)_{\mathbf{R}_0} F_s F_t + \dots \quad (33)$$

$$[H]_{ij} = \left( \frac{\partial^2 G(0, R)}{\partial R_i \partial R_j} \right)_{\mathbf{R}_0} - \sum_s \left( \frac{\partial^2 \mu_s}{\partial R_i \partial R_j} \right)_{\mathbf{R}_0} F_s + \dots \quad (34)$$

By introducing eqs 33 and 34 into eq 29, we obtain the following expansion for the components of the displacement vector  $\mathbf{d}$ :

$$d_i = \sum_s \sum_j [(\mathbf{H}^0)^{-1}]_{ij} \left( \frac{\partial \mu_s}{\partial R_j} \right)_{\mathbf{R}_0} F_s + \frac{1}{2} \sum_{st} \sum_j [(\mathbf{H}^0)^{-1}]_{ij} \left( \frac{\alpha_{st}^e}{\partial R_j} \right)_{\mathbf{R}_0} F_s F_t + \dots \quad (35)$$

where  $\mathbf{H}^0$  is the Hessian of the molecular solute in the absence of the external applied field  $\mathbf{F}$ . In eq 35 we have neglected all the terms deriving from electric anharmonicity, i.e.,  $\partial^2 \mu_s / \partial R_i \partial R_j$ .

From eq 35 we can derive the first and second derivatives of the equilibrium geometry with respect to the field

$$\left( \frac{\partial R_i}{\partial F_s} \right)_{\mathbf{R}_0} = \sum_j [(\mathbf{H}^0)^{-1}]_{ij} \left( \frac{\partial \mu_s}{\partial R_j} \right)_{\mathbf{R}_0} \quad (36)$$

$$\left( \frac{\partial^2 R_i}{\partial F_r \partial F_s} \right)_{\mathbf{R}_0} = \sum_j [(\mathbf{H}^0)^{-1}]_{ij} \left( \frac{\alpha_{rs}^e}{\partial R_j} \right)_{\mathbf{R}_0} \quad (37)$$

and consequently to rewrite eqs 26–28 as

$$\alpha_{rs}^v = \sum_{ij}^{3N} [(\mathbf{H}^0)^{-1}]_{ij} \left( \frac{\partial \mu_s}{\partial R_j} \right)_{\mathbf{R}_0} \left( \frac{\partial \mu_r}{\partial R_i} \right)_{\mathbf{R}_0} \quad (38)$$

$$\beta_{rst}^v = \sum_{ij}^{3N} [(\mathbf{H}^0)^{-1}]_{ij} \left[ \left( \frac{\partial \mu_t}{\partial R_j} \right)_{\mathbf{R}_0} \left( \frac{\partial \alpha_{rs}^e}{\partial R_i} \right)_{\mathbf{R}_0} + \left( \frac{\partial \mu_s}{\partial R_j} \right)_{\mathbf{R}_0} \left( \frac{\partial \alpha_{rt}^e}{\partial R_i} \right)_{\mathbf{R}_0} + \left( \frac{\alpha_{st}^e}{\partial R_j} \right)_{\mathbf{R}_0} \left( \frac{\partial \mu_r}{\partial R_i} \right)_{\mathbf{R}_0} \right] \quad (39)$$

A further development is then achieved by substituting the Cartesian coordinates  $\{R_i\}$  with the normal coordinates  $\{Q_a\}$  which diagonalize the Hessian  $\mathbf{H}^0$ ; in this way we exactly obtain expressions 9 and 10. The parallelism between the two sets of equations is then complete once all the quantities are computed in their respective environment, the gas phase for the isolated system and the solution for the molecular solute.

(51) Bishop, D. M.; Kirtman, B.; Champagne, B. *J. Chem. Phys.* **1997**, *105*, 5780.